32nd Electric Vehicle Symposium (EVS32)
Lyon, France, May 19 - 22, 2019

Battery weight optimization for hovering aircraft

T.Turcksin†, P.Van den Bossche
†*T.Turcksin, Vrije Universiteit Brussel, MOBI-INDI-ETEC, Pleinlaan 2, 1050, Belgium, tom.turcksin@vub.be*

Abstract

In situations where slip is zero (road vehicle modeling), the load cycle can be defined rather simply. The system obeys conservation laws and the energy flows are relatively simple to describe. This eventually results in dynamic system equations used for load cycle simulations.
The case of a hovering aircraft is somehow misleading. The reason for the difference is rooted in the fact that slip is never zero. For this reason, energy is constantly dissipating until there is no more left.
In this paper the simplest approach i.e. an energy analysis is followed. Nevertheless, this will be sufficient to answer one of the most important design questions. " How to determine the battery weight in order to maximize performance?"
Keywords: Vehicle performance, power, energy, mobility concepts, optimization.

1 Introduction

1.1 Acronyms and symbols

Table 1: list of symbols and acronyms

e_b	Specific energy	eVTOL	Electric vertical takeoff and landing
η_{tot}	Total efficiency	DEP	Distributed electric propulsion
η_{prop}	Propulsive efficiency	ESC	Electronic speed control
η_{eff}	Effectiveness	3S or 4S	Three or four cell battery pack
m_s	Mass structure	BLDC	Brushless direct current motor
m_b	Mass battery	RC	Radio Controlled
Δt	Endurance	HAV	Human sized Aerial Vehicle
A_p	Propeller area	AC	Aircraft
ρ	Air density	MTOW	Max take off weight
P	Power	EW	Empty weight
F	Developed thrust force		
C_L	Lift coefficient		
C_D	Drag coefficient		
v_i	Velocity at section i		
section a, p, s	Free stream, propeller, jet		

1.2 Context

Air and noise pollution are among the main drawbacks of todays aircraft. Electrically propelled aircraft address these two problems in a significant manner. Policies and markets are moving towards this direction. For example, Norway has committed to have all their domestic flights electrically propelled by 2040. [7].

1.3 A matter of scale or synergy of technologies?

Small multi-copters have been around for several years. They are taking care of many inspection-related tasks. It seems that in the small scale, RC market segment, electrically powered aircraft is the standard. However larger AC are equipped with turbo engines in most of the cases.
The reasons for this difference in technologies is twofold:

- Lift and drag forces are applied on a surface while weight is a body force. Therefore the feasibility of a VTOL aircraft is inversely proportional to the square root of the characteristic length. So at small scale a drone intrinsically requires less energy-dense technology. This also shows that at a large enough scale a solution with a thermal engine of some kind will probably remain necessary for a while.
- Let us assume a high energy lithium cell with energy density of 200 Wh/kg. This is about 60 times less compared to the 45 MJ/kg stored in Kerosene. The efficiency of a thermal motor is much lower than what is achievable with electric power-trains but it does not make up for the difference.

Luckily, for human sized, electric VTOL concepts, the feasibility does not relay on batteries alone to provide the required range and endurance. Aircraft designers can use several tools for VTOL capability estimation:

- Disk loading[1]: Propulsive efficiency is often defined as $\eta_{prop} = v_a/v_j$ [4]. It is clear that a larger discharge area (and consequently lower disk loading) allows for higher propulsive efficiency. This is the idea behind distributed propulsion. High bypass turbo fans utilize this approach to increase efficiency and reduce noise. However, for practical reasons distributed electric propulsion or DEP more easily exploits this effect. The NASA GL-10 is a good example. Work by Mark Moore on DEP [6] also demonstrated additional benefits with respect to boundary layer control.
- Glide ratio[2]: According to the white paper from Uber, the glide ratio should be higher than 10, preferably between 12 and 17. [3]. The addition of a wing is therefore crucial for range and endurance. For VTOL (considering only steady state conditions), the degree of load modulation should be of the same order as the glide ratio of the aircraft (also known as the maximal aerodynamic efficiency[3]). So VTOL aircraft with cruise capabilities clearly require a power train with good modulation characteristics. In comparison to thermal-turbo-engines, electric power trains excel at this.

Figure 1 illustrates power and disc loadings for some thermal, electrical and hybrid power train VTOL aircraft. The power levels are averaged values. The presented chart results from public data. Because this does not always comes in a very structured way, the chart should be taken with a small grain of salt. For instance, for the Vahana Alpha, propeller area was deduced from the figures in [9]. The mass is calculated as the average of the MTOW and EW which allows to find the disk loading. The average power was found assuming a energy density of 200 Wh/kg. Along with a battery weight of 272 kg, a range of 60 km and speed of 200km/h [9] an average power of 180 kW. Significantly less than the available 360 kW peak power (limited by the motors) and so a value for power loading is extracted.
Before going any further, a theoretical distinction between jets and props is due. In the aeronautical industry a big difference exists between these two propulsion systems [4].
Aircraft propulsion is typically a turbo engine, by default these are air-breathing thermal engines. If we consider a turbo jet, then the inlet air flow is proportional to the fly velocity. If the stoichiometric ratio of the air-fuel mixture is kept constant, the power should increase with fly velocity. This effectively leads to a constant thrust device. On the other hand, for turbo props, the air intake is situated behind the propeller. So even if the aircraft is at standstill the air intake is situated at a location where the air velocity is equal to the down-wash velocity. If the propeller aircraft gains in speed, the velocity at the intake won't change significantly leading to the constant power or so called propeller idealization.
For electric fans this distinction does not apply. Instead the choice of idealization depends on the power and disk loading. If these values are high enough, the jet idealization applies, if they are low, a prop idealization is more appropriate. Due to DEP, eVTOL HAV can typically be described with the propeller idealization resulting in high available thrust at takeoff and lower thrust in cruising conditions. In relation to figure 1, the AC on the left have a propeller propulsion system while those on the right tend more towards the jet idealization. .

[1] Disk loading is defined as thrust over discharge/propeller area and expressed in pascals

[2] The Glide ratio is the maximal aerodynamic efficiency

[3] The aerodynmic efficiency C_L/C_D is function of the angle of attack (flaps and slats in retracted position).

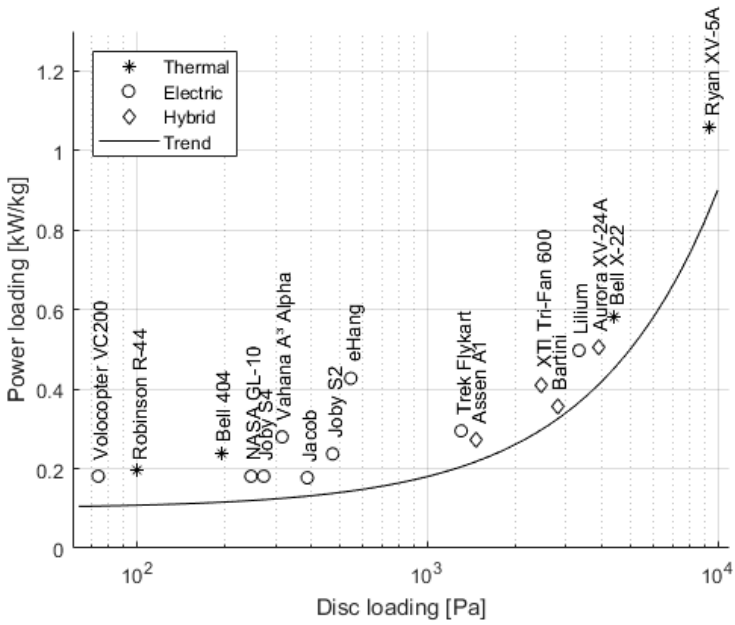

Figure 1: Power and disk loading [3], [1], [9]

Figure 2: Lilium aero, MTOW 640 kg [1] [9]

Figure 3: Vahana Alpha, MTOW 726 kg [14] [9]

1.4 The case of eVTOL AC

The increasing capabilities that electric motors offer in combination with battery and inverter technology allow for the creation of a new type of electric VTOL aircraft. Examples are the Vahana [14] (figure 3), or Lilium [1] (figure 2). Today more than one hundred examples are already listed on the eVTOL.news website [9]. It is clear that technological feasibility is not the issue anymore. However, besides the power limitation, we should consider the practical limitation (energy wise). This translates in a limited endurance especially for the battery powered aircrafts. Also, social questions arise; is society ready to accept flying cars? What about noise, pollution and sustainability? Will future crashes of HAV eVTOL aircraft be marginalized as road vehicle crashes or will they continue to be world wide front-page news? These questions are essential and might shake the aeronautical sector in very unpredictable way.

Classification of eVTOL Within the electric vertical take off and landing human sized aerial vehicle or in short eVTOL HAV, one can differentiate between five sub categories [9]:

- Vectored thrust: An eVTOL aircraft that uses any of its thrusters for lift and cruise.
- Lift + Cruise: Completely independent thrusters used for cruise as for lift.
- Wingless (multicopter): No thruster for cruise only for lift.
- Hover bikes/devices: These eVTOL aircraft are considered to be in the general class of hover bikes, with the primary differentiation being that the pilot sits on a saddle.

- Electric helicopters: An electric aircraft that utilizes helicopter flight controls (cyclic, collective, etc.).

1.5 Scope of this paper

This paper analyzes the impact of the battery weight on the endurance Δt of a statically hovering eVTOL. Simplifying the equations and models will lead to a very simple rule.
For validation, tests have been performed with a drone. The test results are compared to the theoretical results and conclusions are drawn.
The optimization procedure proposed in this paper is limited to Wingless eVTOL applications. However, the proposed results allow for an unknown constant efficiency. Thus as long as the averaged efficiency can be considered independent of a change in battery weight, this optimization procedure should apply. This indicates that the proposed optimization procedure and results can be more widely applied in eVTOL applications.

2 Jacob the test robot

2.1 General description

To verify the model, a concrete test platform is required, therefore a testing drone Jacob (depicted in figure 5) was built. In order to learn from the build-up, separate parts were purchased.
The structure (from DJI®) comes in a package together with the ESC's, motors and propellers. The radio transmitter and receiver is the DEVO10 from Devention®. To use it, the transmitter is loaded with latest Deviation® software. The transmitter offers ten channels that can be programmed in many different ways. The DEVO10 is mostly used for helicopters and airplanes. For the multicopter layout used in this project, a separate flight controller equipped with orientation and displacement sensors is needed: the Atom® CC3D flight controller. Besides measuring orientation and displacement, the atom takes in airplane commands (aileron, rudder, throttle etc.) from the DEVO10 receiver and uses both sensor and command data to generate the control signals driving the ESC's. The CC3D flight controller also allows to connect other peripherals such as a camera or GPS sensor. CC3D comes with ground station software.
The final piece is the battery. Based on experience of the salesman, 3S battery packs have been chosen. As the ESC's are rated up to 15.5 Vdc, 3S packs seemed the right choice (4S packages can reach up to 16.8 Vdc). However, it seems the voltage regulator of the ESC's is unable to produce the 5 Vdc voltage needed for the Atom and radio receiver. Because no information could be found w.r.t. the power consumption of the receiver and because the goal was to analyze the power flow in the drone, a separate fully monitored feeder to power all electronics (monitoring devices, flight controller and radio receiver) was installed.
After some experiments, we realized that at the end of a fly cycle and some relaxation time, cell voltage would reach about 3.7 Vdc. Although the batteries were able to bring the drone up into the air only a relatively small part of the actual charge was used during flight. In the end, 4S battery packs were purchased as well. Due to the previous experiences with the 3S packs (capacity reaching only 88% of rated capacities) Turnegy® (a well established brand) were chosen. In contrast to the 3S pack, the cell voltages of the 4S packs reached 3.4 Vdc after some relaxation time. Indicating the discharge cycle was able to deplete the cell much further.

2.2 General parameters

An overview of the parameters used in the optimization problem is given in this section.
The mass of Jacob with all additional measurement devices but without the battery is measured to be 1060 ± 5 gr.

Propellers The propellers or fans are driven by the brushless DC(BLDC) motors. The conversion of electric power to thrust can be rather complicated however in this paper the simplest model for thrust is used. The only required parameter is the propeller's surface area. The propellers have a hub and tip radius of respectively 20 and 112 mm. The available propellers are also characterized by their pitch (4.7 in this case). This parameter is not jet reflected in the model.

ESC The motors are driven by the electronic speed controllers or ESC. Many differences between ESC's exist. Depending on the ESC/motor combination, a particular efficiency can result.

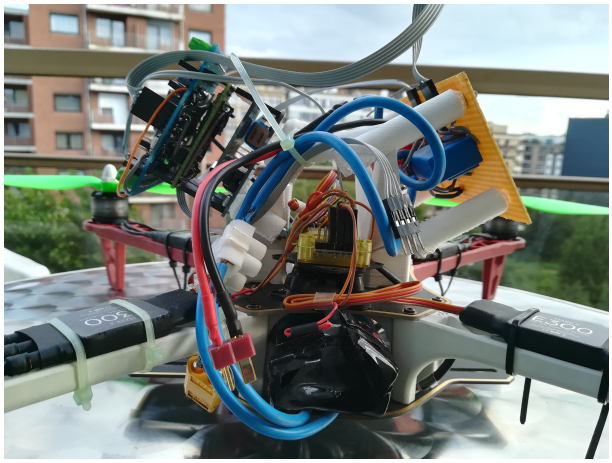

Figure 4: Close-up logging station

Figure 5: Test-setup

Motors The motors are typical brushless DC's. These motors are known to yield a very high specific power. They have a kV-rating of 920 kV. A kV unit expresses the number of no-load rpm achieved per applied DC volt. It is inversely proportional to the more common "$k.\phi$" value used in the theory of DC motors ($T = k.\phi.I$ and $E = k.\phi.\omega$).

Battery specifications Several battery cells were used in this study. The main data of these is reported in table 2. Due to inaccuracy of the provided data, the energetic capacity has been measured in separate tests using professional equipment (CTS® climate chambers and PEC® battery tester). A capacity check was performed according to the IEC-62660-1 standard.

Table 2: Verified battery properties.

Name of pack	cell count	capacity [Ah]	weight [gr]	energy density [Wh/kg]
Turnigy® 3	4	3	380	117
Turnigy® 4	4	4	453	131
Turnigy® 5	4	5	574	129
Turnigy® 3-4	4	7	833	
Turnigy® 4-5	4	9	1027	

From the obtained results, one can conclude that the energy densities of all packs are approximatively the same: 126 Wh/kg. This is certainly not the highest energy density achievable, in fact one pack that was excluded due to inaccurate data from the supplier presented a (verified) energy density of about 157 Wh/kg. Today some manufactures like Solid-Energy® are reaching 381 Wh/kg energy density [2] at 3 It discharge rates.
The verified results presented in table 2 are at pack level so the weight includes the connector and wires, part of the battery pack assembly. The last two lines in table 2 are combinations of two other packs. Special cables were manufactured to connect packs and individual cells in parallel.

2.3 Onboard measurements

An Arduino® Uno is used to perform and store measurements. The micro processor monitors the individual cell voltages, the current powering the ESC's and the current powering the on-board electronics. The data is saved locally on an Sd-card. The sample rate can be set by the operator to a maximal value of 40 Hz. All measurements are isolated using optocouplers except for the ESC current measurement where isolation is achieved through a compensated Hall sensor.

Voltage measurements The cell voltages are individually monitored through optical isolation components. The 4N35 was used for this purpose. To ensure that the operation of the optocouplers captures the measurement range we are interested in, an additional diode was installed on the battery side. For measurements between 3 and 4.5 Vdc, the achieved voltage measurements are accurate up to ± 0.1 Vdc.

Current measurement for electronics To measure the current drawn by the electronics a small shunt (0.5 Ω) was installed. The voltage signal over this shunt was amplified through an inverting amplifier after which it passes through the optocoupler. Verification of the calibration demonstrated an accuracy of 0.01 A for currents between 0.18 and 0.5 A.

Current measurement The current measurement was calibrated on currents up to 30 A, they were proven to be accurate up to ± 0.2 A when compared to an external measurement. Because the LEM sensor is based on the hall effect, the measurement is isolated by default.

3 The simplest approach for batteryweight optimization

For conventional aircraft, a distinction is made between range and endurance optimization. The differentiation is a consequence of the loss in mass during flight. A fully loaded conventional passenger aircraft can approximatively lose one third of its takeoff mass during the flight. This in turn results in a lower angle of attack leading to less drag and therefore a significant increase in range.
In the case of a battery powered aircraft, the weight of the aircraft remains constant. This simplifies the equations and the distinction between range or endurance optimization as applicable for conventional combustion powered aircraft is no longer relevant.

3.1 Conclusions of thrust model

Based on previous work from [4], [10], [5] and [11], we can deduce the propulsive force of an ideal propeller. A small recitation of the important concepts, assumptions and conclusions of that work are given here.

Assumptions of thrust model: The following assumptions are made in the model.

- Bernoulli considers incompressible fluid. This assumption for air is valid if the pressure perturbations remain minor and the velocity remains under Mach 0.5 [4].
- Bernoulli assumes inviscid fluids, which means no friction losses. The viscosity of air is rather low (18.1 $\mu Pa.s$ [13]) which motivates this assumption but at high velocities frictional effects can play an important role.
- The process is considered adiabatic therefore the airflow does not undergo any temperature changes.
- The process is considered isentropic and thus reversible.
- Since the propeller model has no physical surfaces, there is no surface for drag to develop on. So no pressure drag or friction drag.
- All power is evenly distributed over the propeller area and transformed into rise in impulse.

Stream fields and control volumes In the analysis of fans, a good representation of the stream is key. The stream tube for a propeller in hovering and forward flight condition is illustrated in figure 6. The stream that flows through the propeller is confined to a three dimensional stream-tube. The part of this stream-tube, reaching from section a to section j will be used as control volume on which the conservation laws can be applied. This underlines the importance of an accurate definition on the location of the ambient and jet sections respectively denoted with letter a and j.
We make a distinction between three sections; the ambient section, the propeller section, and the jet section. It is important to understand that the ambient section lies somewhere upstream, where the ambient air stream is unperturbed. The jet section lays somewhere downstream where the air is fully expanded, this is typically not very far from the fan. It is clear that the exact location of these sections remain function of the ambient velocity field and the working regime of the propeller. Also these sections can always be described with a plane surface.
In general one can say that the area of the upstream section (the unperturbed section), increases with power and decreases with $\vec{v}_a = \vec{v}_{wind} - \vec{v}_{aircraft}$. If the ambient velocity v_a is high enough, then the upstream stream-tube tends to diverge a bit before reaching the duct. This leads to spillage drag and lip-suction effects [8]. As it requires compressible fluid, this reaches out of the scope of the paper. Therefore, we will only consider low speeds (i.e. < 0.5 Mach).
The stream tube can take on several distinct shapes, as illustrated in figures 7 and 6:

- In the second image of figure 6, the propeller is in a uniform downward wind profile. Since energy is added to the flow, velocity will increase. Due to conservation of mass one knows that the flow must converge. The area of the unperturbed surface becomes larger than the propeller area.

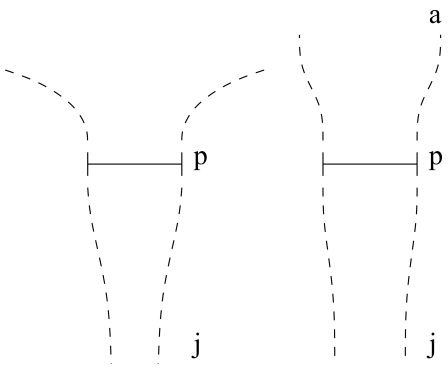

Figure 6: Stream-tubes in hover and climb.

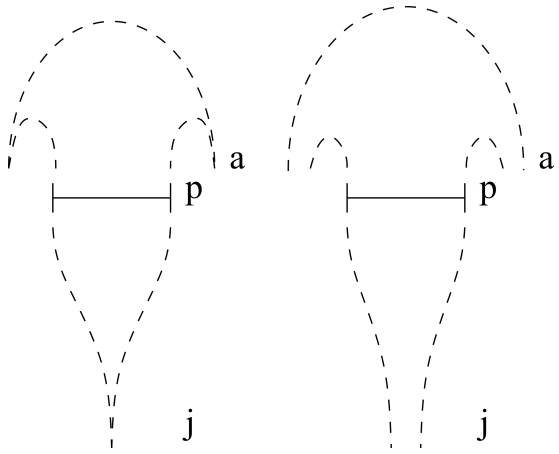

Figure 7: Stream tube for a fan in backwind

- The left image of figure 6 depicts a duct ready for vertical takeoff, here the ambient air stream at the unperturbed section is zero, at the same time, the surface area at the unperturbed air stream becomes infinite.
- If we further decrease the ambient velocity such that v_a becomes negative, the upstream stream-tube changes in a drastic manner (see right illustration in figure 7). A net mass flow will stream from section a to j. If v_a becomes even more negative or if power is decreased further, the mass flow through the fan will get blocked. Because the mass flow is zero, no thrust can be developed.

With these physical illustrations in mind we now know to which volume the conservation laws can be applied. This introduction also indicates a potential pitfall. Since a single propeller section is considered, no distinction is made between the velocity just before and just behind the propeller. Notice that this model does allow for different total pressures, in fact equation 2 results from this property.

The propulsion equation The Bernoulli equation can be applied two times, once on a stream line, from section a to section p, a second time it can be applied to a stream line leaving the duct form section p to j. The Bernoulli equation is not valid over the propeller because in section p, total pressure is added. These two equations can be combined to yield an equation for thrust (left side of Eq. 1).

Conservation of momentum can also be computed over the control volume (reaching from section a to j). This leads to a second formulation for thrust. Equating both expressions leads to a relation between the velocities (or, due to the incompressible fluid, the surface areas) at the different sections (right side of Eq. 1).

$$\frac{1}{2}.\left(v_j^2 - v_a^2\right) \overset{Ber.}{=} \frac{F}{\rho.A_p} \overset{Mom.}{=} v_p.\left(v_j - v_a\right) \tag{1}$$

or,

$$v_p = \frac{v_j + v_a}{2} \tag{2}$$

This equation gives us information on the shape of the considered stream tube and tells how the ideal propeller works.

Conservation of energy Because of the assumptions made, introducing a power source is quite simple. It is sufficient to represent it as a gain in total pressure or a force times velocity.

$$P = A.v_p.\frac{\rho}{2}.\left(v_j^2 - v_a^2\right) = \rho.A.v_p.\left(v_j - v_a\right).v_p \tag{3}$$

One can also consider it as a gain in kinetic energy per second for the mass flowing through the propeller. Substituting relation 2 in this last equation leads to the following cubic formula.

$$0 = v_j^3 + v_a.v_j^2 - v_a^2.v_j - v_a^3 - \frac{4.P}{\rho.A_p} \tag{4}$$

Solving this polynomial for v_j allows to subsequently calculate thrust with the equation of Bernoulli or momentum.
It is interesting to note that equation 4 has possibly three real roots and certainly one real root. In practice however, if all values are positive, only one real root exists. To allow for negative values of v_a, the last equation can be rewritten to:

$$0 = v_j^3 + v_a.v_j^2 - \frac{v_a^3}{|v_a|}.v_j - v_a^3 - \frac{4.P}{\rho.A_p} \tag{5}$$

And again only one real root will exist. This last step is only necessary for propellers that are placed in a uniform air stream with a propeller blowing in the opposite direction.
The model introduced in [11] is very similar but the difference is that, they already accept a certain load force and then compute the required power to achieve it. With this approach the opposite is done, we accept a certain power and compute the available thrust resulting from it.

3.2 Battery weight optimization

Hovering power and thrust. In the following part we will consider the simplest case, namely the case where the aircraft is hovering on a fixed position in a wind still environment $v_a = 0\,m/s$. In this particular case, the equations are simplified to yield the following relations.

$$v_a = 0 \tag{6}$$
$$v_p = v_j/2 \tag{7}$$
$$F = 2.v_p^2.\rho.A \tag{8}$$
$$P = 2.v_p^3.\rho.A \tag{9}$$

The last equation allows to directly compute v_p from the input power and propeller area. This can then be substituted back into the propulsion force equation yielding the following simplified equation relating thrust and power.

$$F = (2.\rho.A_p)^{1/3}.P^{2/3} \tag{10}$$

or

$$P = \frac{F^{3/2}}{(2.\rho.A_p)^{1/2}} \tag{11}$$

Formula for endurance From a practical point of view, it seems straight forward to optimize endurance. Thus an equation for endurance is needed. By equating the required and available thrust (eq: 10), one gets:

$$(m_s + m_b).g = (2.\rho.A_p)^{1/3}.P^{2/3} \tag{12}$$

furthermore assuming the battery behaves as an ideal voltage source with finite capacity,

$$\Delta t.P = \eta_{eff}.m_b.e_b \tag{13}$$

one easily finds an equation for endurance, denoted here with Δt:

$$\Delta t = \frac{\eta_{eff}.e_b.\sqrt{\rho.A_p.2}}{g^{3/2}}.\frac{m_b}{(m_s + m_b)^{3/2}} \tag{14}$$

Battery weight optimization Let us consider a hovering aircraft. The question arises, how large should the battery be to yield the best performance? An even more important question, what is performance? Efficiency is clearly ill-defined because the useful power output is calculated as $F.v_a$ and since the aircraft has a fixed position and no wind is assumed $v_a = 0$, the output power and efficiency are zero.

Performance indicators can be defined in arbitrary ways. Important in this approach is to be aware of their holistic implications. For instance optimizing endurance may lead to higher required power. Which in turn may require better cooling and a more powerful system. In the following we choose to define two performance indicators and compare the resulting design criteria after optimization.

For illustrative purposes, the influence of the design parameter m_b/m_s on the performance indicators defined below is illustrated in table 3.

Available endurance The optimization criteria for endurance can be met by differentiating equation 14 towards m_b and equating it to zero. This leads to:

$$m_b = 2.m_s \tag{15}$$

This result is independent of propeller size, aircraft size or battery technology. An important assumption however is that the total averaged efficiency remains constant for changing m_b.

From table 3, we notice that an optimization for endurance alone makes little sense. In fact doubling the battery size from m_s to $2.m_s$ will only result in 8% more endurance. Another optimization criterion might be more desirable.

Available endurance over required power Let us now consider the drone is limited in power. So the optimization criterion can be redefined. One want to maximize the available endurance while minimizing the required power.

$$\frac{\Delta t}{P} = \frac{\eta_{eff}.e_b.\rho.A_p.2}{g^3}.\frac{m_b}{(m_s+m_b)^3} \sim \frac{\Delta t^2}{m_b} \tag{16}$$

Differentiating this towards m_b yields an optimal battery size:

$$m_b = \frac{1}{2}.m_s \tag{17}$$

From table 3 one can notice that this second optimization criterion is more suitable. (Practically speaking I do not think that Jacob will be able to handle the three times higher required power output needed to fly in $m_b = 2.m_s$ configuration.) This "design rule" is actually applied in several existing concepts for example the Vahana [9].

Table 3: Normalized performance indicators as function of m_b/m_s

m_b/m_s	2	3/2	1	2/3	1/2	1/3	1/4
P/P_{max} [%]	100	76	54	41	35	30	27
$\Delta t/\Delta t_{max}$ [%]	100	98.6	91.9	80.2	70.8	56.2	46.5
$(\Delta t^2/m_b).(m_b/\Delta t^2)_{max}$ [%]	50	65	84	97	100	95	86

This section, proves that the battery should never make up more than 2/3 the total weight of the aircraft. A higher weight will only decrease endurance leading to useless weight, overpowered systems, and higher discharge rates.

Also it is proved that optimizing endurance alone is not the most suitable approach. In fact doubling the battery weight from $1.m_s$ to $2.m_s$ only yields a very expensive 9% endurance increase while the required power will increase by a factor of 185% (100% corresponding to the performance achieved for $m_s = m_b$).

3.3 Effectiveness a special type of efficiency

We know that the total efficiency of a drone is zero. However since efficiency is obtained from a multiplication of a whole string of factors, it is easy to imagine only one η_{prop} will be zero in static hovering flight. So although the efficiency is zero, it does not mean that all other factors of the total efficiency are zero.

$$\eta_{tot} = 0 = \eta_{eff}.\eta_{prop} \tag{18}$$

Since optimization of total efficiency did not make sense, another mathematical indicator has to be defined. Instead of comparing powers, it makes sense to compare the real achievable endurance to the theoretically achievable endurance. We define this parameter as effectiveness and denote it with η_{eff}.

$$\eta_{eff} = \frac{\Delta t_{real}}{\Delta t_{ideal}} = \frac{\eta_{tot}}{\eta_{prop}} = \frac{\Delta t_{real}.g^{3/2}}{e_b.\sqrt{\rho.A_p.2}}.\frac{(m_s+m_b)^{3/2}}{m_b} \tag{19}$$

It is interesting to note that in equation 14, an efficiency factor comes forward. This efficiency is not the total efficiency (nor is it zero). To make a distinction, we call this efficiency, effectiveness.

The model introduced in previous section is ideal. Another way of understanding it is by considering an ideal propeller. Instead of defining the output power as $F.v_a$, one should define the output power locally as $F.v_p$. This along with the rule for an ideal propeller $v_p = (v_a + v_j)/2$ yields the formula for propulsive efficiency applicable to any condition (cruise or hovering) [5].

$$\eta_{prop} = \frac{F.v_a}{F.v_p} = \frac{v_a}{v_p} = \frac{2}{1 + \frac{v_j}{v_a}} \tag{20}$$

This means that the effectiveness of a drone can easily be calculated by comparing the real and theoretically achievable endurance as shown in equation 19. In my opinion it is obviously a key figure of merit that deserves some recognition as it is the next best thing after efficiency. The effectiveness encompasses all other efficiency factors apart from the propulsive efficiency and for that reason is non zero in the static hovering condition. So in fact effectiveness is the factor that can and should be optimized in hovering applications.

4 Experimental validation

4.1 Measurement campaign

With each battery pack, an endurance test was performed. The measurements were done outside on a calm and windless day. During the flight we tried to keep the drone steady at a height of approximatively five meters. This clearance allows to reason out the ground effect.

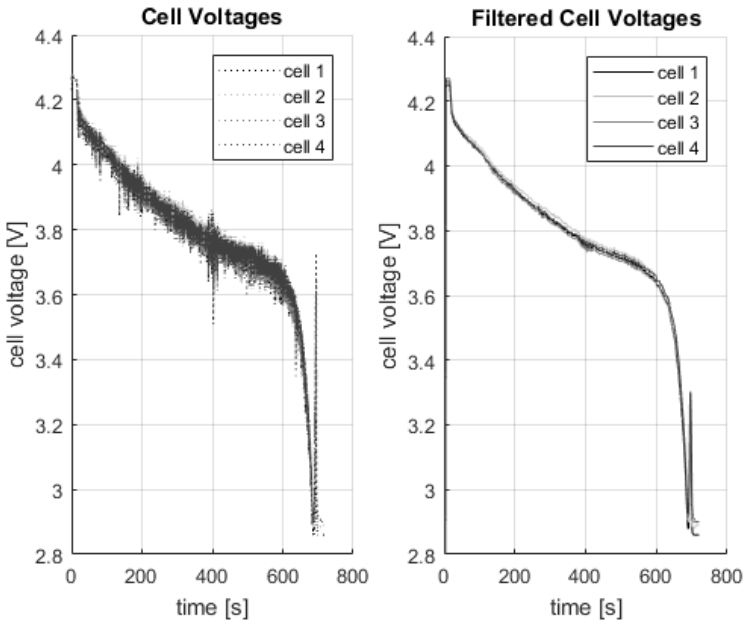

Figure 8: Cell voltages

The measured signals from the 4S 3Ah battery pack are depicted in figures 8, 9 and 12. The data presents some noise, we can crisp the image by using a moving average filter. Here 200 frames are combined to create a smooth signal.
The electronic current, see figure 9 on the right, accounts for the receiver, the flight controller, the Arduino and the diverse sensors connected to it. Several remarks are in order. One can notice that no values under 180 mA are depicted. This is due to the dead zone (voltage wise) introduced by the isolation circuit. For this reason a minimal signal of 180 mA is always measured. A second remark is that there is a clear correlation between the current measured for thrust and the current absorbed by the electronic circuit. This is caused by the LEM current sensor which consumes a reasonable amount of power compared to the other electronic components.
From these signals we can easily compute the power to drive the electronics and the power to generate thrust. The total power can be integrated to yield energy. This is depicted in figure 10. The average measured power and endurance can be estimated. This is done for each battery pack. The results are shown in table 4.

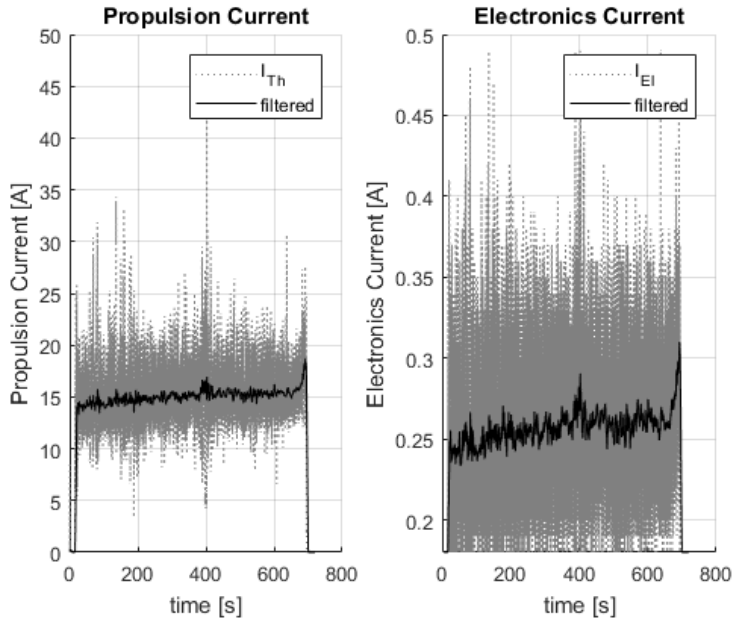

Figure 9: Current, left for thrust development, right electronics supply

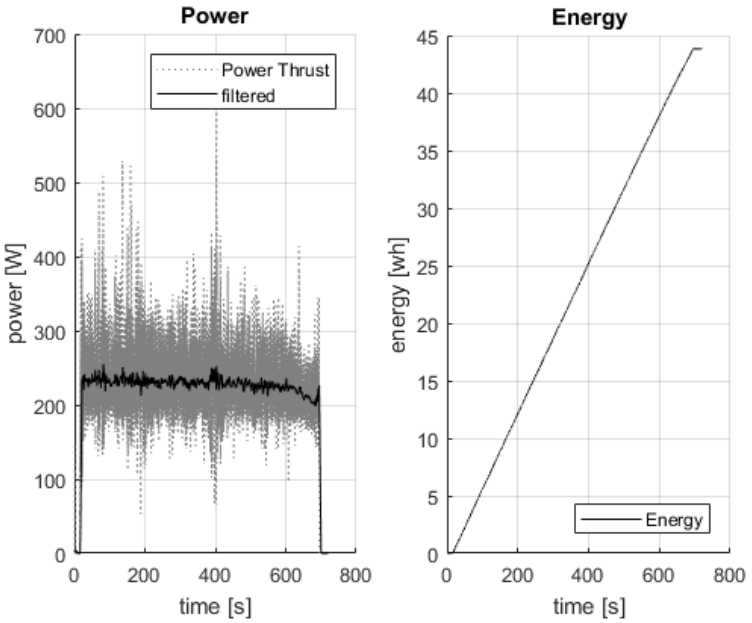

Figure 10: Power and energy computation

Name of pack	Weight [gr]	Power [W]	Endurance [s]
4S Turnigy 3	380	244	653
4S Turnigy 4	453	274	780
4S Turnigy 5	574	320	830
4S Turnigy 7	833	385	968
4S Turnigy 9	1027	446	1073

Table 4: Measured performance of test flights ($\pm$ 10 W, $\pm$ 10 s).

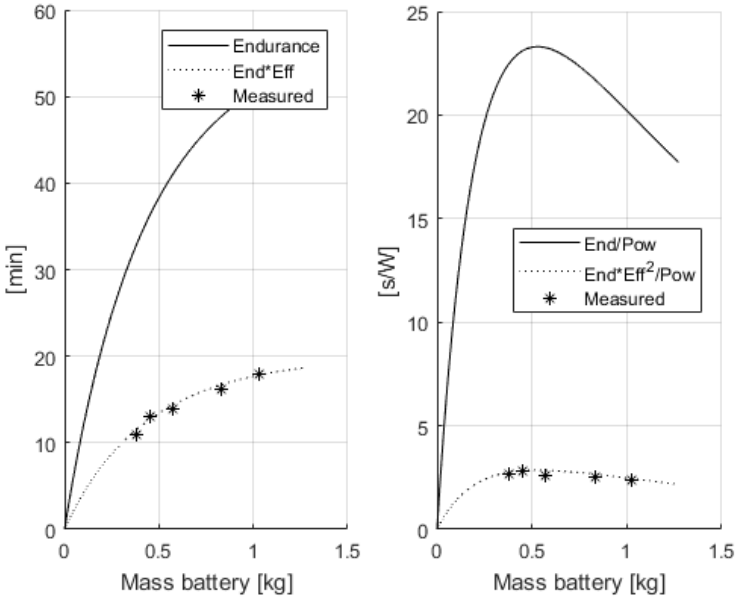

Figure 11: Endurance

Model validation Model validation is performed by comparing the theoretical model to measurements. Direct validation of the $m_b = 2.m_s$ rule is difficult. We can expect that Jacob, by itself weighing 1 kg, might have difficulties carrying an additional 2 kg of batteries. Moreover the motors are limited to about 200 W each, and only a large enough safety factor ensures reactive dynamic behavior needed for control. For these reasons the focus is given to the second optimization parameter: the endurance to power ratio. In practice, the validation can only be performed indirectly. It translates in the verification of the location of the peak in the figure 12 (right side). So only the evolution of the performance indicators can be predicted. The dots must lie on a curve as predicted by the model, but this curve can be a scaled dawn version to encompass for a fixed but smaller than unity effectiveness factor. In other words, the difference between theory and model is a direct measure for the effectiveness.
It is important to verify the accuracy achievable on the measured total efficiency. We note that even though a lot of care is taken with respect to the numerical values, an accuracy of around 6% can be achieved at best. The inaccuracy of the electric variables has probably the highest impact.
Most parameters are determined with an accuracy up to 1%. In that regard, the density of air varies more with temperature than with humidity, so using the following first order approximation, for air density at sea level with 50% humidity ($\rho\,[kg/m^3] = 1,2947 - 0,0045.T[^\circ C]$), density can easily be approximated if the temperature is known [12].
Indeed a small peak can be seen on the right plot of figure 11. We can also recognize the increase in endurance in the left plot. For this reason the validation results are rather positive. Scarce data and numerical tolerance makes it difficult to draw hard conclusions but besides that the results are as expected.
Figure 12 illustrates the effectiveness of the propeller. In this case we can see that it is rather constant and around 35%. This is rather poor, but then again Jacob was not constructed to be efficient. The 65% losses are due to, heat generation in the battery, the ESC, the motor and the carrying fluid. Besides all dissipative terms there is also the fact the produced impulse stream is having a rotating component and in general is not fully aligned with the propellers'axis. Finally my personal flying capabilities are not excellent and perhaps the controller was not perfectly optimized leading to more unnecessary movements.

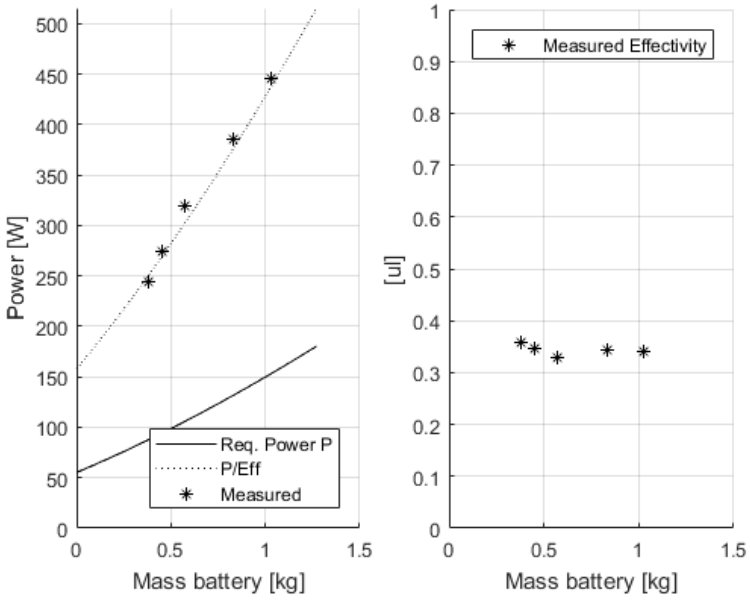

Figure 12: a) Power of model and Real power b) Effectivity

4.2 Conclusion

In this project, drone efficiency was examined. It was demonstrated that effectiveness is a better measure because unlike efficiency, it is not zero in static hovering condition.

- The most important result is equation 14 which allows to compute the endurance for hovering aircraft.
$$\Delta t = \frac{\eta_{eff}.e_b.\sqrt{\rho.A_p.2}}{g^{3/2}}.\frac{m_b}{(m_s+m_b)^{3/2}}$$
- The second most important result is that endurance can not increase further when the battery makes up 2/3 of the total weight. This results from a mathematical limitation independent of physical parameters.
- We proved that optimizing endurance alone is not the best approach. In fact doubling the battery weight from $1.m_s$ to $2.m_s$ only yields a very expensive 9% endurance increase while the required power will increase by a factor of 185% (100% corresponding to the performance achieved for $m_s = m_b$).

On the practical level, the next step for this research is to develop a better electronic logging station with higher sample rate and more analog inputs. This may allow to log other data like position, temperature and orientation. Getting familiar with existing telemetry capabilities and better flight controllers may prove to be very useful.

Better and more data will allow to test more interesting models. For now the verified model corresponds to the static hovering case. Some important design parameters (propeller pitch and camber) are not even matter in the proposed model.
In the future, the model should be expanded to reside in a three dimensional space. Also making use of the pitch and camber parameters shall be done because their addition will lead to a fully dynamic model, i.e. it allows to accurately predict the power couples (torque-pulsation, voltage-current, thrust-propeller velocity). Being able to fix torque and pulsation independently (not just their product) will be a big step forward as efficiency maps are typically defined as a function of both metrics.
The results of this holistic energy analysis are based on very simple models for each component, however the result is so fundamental and important that the a single paper presenting it as a whole is important for scientists, drone pilots and other drone enthusiasts.

References

[1] LiLium aero®. Simplicity was our most complicated goal, 2018
https://lilium.com/technology/

[2] Solid energy®. *Hermes, high energy rechargeable cells for space, 2017*
http://assets.solidenergysystems.com/wp-content/uploads/2017/09/08171937/
Hermes_Spec_Sheet1.pdf

[3] Goel Nikhil Holden Jeff et al. Uber® Elevate. *white paper*, 2016, p18, 20, 37
https://www.uber.com/elevate.pdf

[4] Patrick Hendrick. *Aircraft propulsion* PUB, Cours universitaire 2013, ULB, p58

[5] Jhon D. Anderson. *Aircraft Performance*, MC GRAW, 1999, ch.3:p.145-150
ISBN: 978-0-07-070245-5

[6] Mark D. Moore, *Distributed electric propulsion (DEP) aircraft*, 2012
https://aero.larc.nasa.gov/files/2012/11/Distributed-Electric-Propulsion-Aircraft.pdf

[7] Dag Falk Petersen, Nordic EV summit Oslo 02/02/2018, *The future of aviation*. Avinor®
https://www.tu.no/filer/EVENT/Nordic_EV_Summit_2018/Dag_Falk-Petersen__Avinor_.pdf

[8] Saeed Farokhi. *Aircraft Propulsion, 2nd edition*, Wiley, 2014, ch.3:p.125
ISBN: 978-1-118-80677-7

[9] Vetical Flight Society, *Electric VTOL news*, http://evtol.news/

[10] T.Turcksin *The airquad, A conceptual and performance analysis*, Thesis, 2013, VUB, ch.2:p.75-81.

[11] Wayne Johnsin. *Rotorcraft Aeromechanics, Branch of NASA Ames Research Center*. Cambridge university, 2013, ch.3:p.39-44 ISBN: 978-1-139-23565-5

[12] Jhon M. Cimbala, Yunus A.çengel. *Fluid Mechanics, Fundamentals and applications*, Mc Graw Hill, 6th edition, Appendix, 2010, ISBN: 978-007-128421-9

[13] Michael A. Boles, Yunus A.çengel, *Thermodynamics, an engineering approach*, Mc Graw Hill, 6th edition, 2007, Appendix, ISBN: 978-007-125771-8

[14] Airbus®, Zach Lovering, 2018, *Vahana's first flight a success*
https://vahana.aero/vahanas-first-flight-a-success-ade26d26ba02

Authors

Tom Turcksin graduated as industrial engineer from the Erasmus Hogeschool Brussel and as aeronautical engineer from the Vrije Universiteit Brussel. He is currently active as researcher within the MOBI research group at VUB. He is focusing on thermal management for high strain battery packs. In particular he investigates the specific obstacles as well as opportunities in the domain of electrically propelled aeronautical applications.

Peter Van den Bossche, civil mechanical-electrotechnical engineer, promoted in Engineering Sciences from the Vrije Universiteit Brussel on the PhD thesis "The Electric vehicle, raising the standards". He is currently lecturer at the Vrije Universiteit Brussel. Since more than 15 years he is active in several international standardization committees, currently acting as Secretary of IEC TC69.